Disentanglement and Crazing in Glassy Polymers

C. J. G. Plummer and A. M. Donald*

Cavendish Laboratory, University of Cambridge, Madingley Road, Cambridge CB3 0HE, U.K.

Received December 16, 1989

ABSTRACT: Deformation mechanisms involving disentanglement by reptation are, in general, expected to be favored over other mechanisms by low molecular weights, low strain rates, and high temperatures. There is overwhelming evidence that crazing in relatively low molecular weight glassy polymers in a regime just below the glass transition temperature, T_g, is also favored by low molecular weights and low strain rates and, further, that the deformation ratio of the crazed material increases with decreasing molecular weight and strain rate in this regime. This has led to models for crazing kinetics that incorporate the possibility of entanglement loss by reptation at sufficiently high temperatures. In this paper we argue that the "block and tackle" mechanism for forced reptation first described by McLeish et al. is appropriate to disentanglement crazing in glassy polymers and examine the consequences of this for craze propagation kinetics.

1. Introduction: Craze Propagation Kinetics

Kramer and co-workers first showed that entanglement loss was of crucial importance for crazing in their work on ambient temperature crazes in low entanglement density polymers such as PS (polystyrene). This may be rationalized with reference to Kramer's model for craze widening,[1] illustrated in Figure 1, craze widening being generally accepted to control the rate of craze propagation into the bulk polymer. The fact that the craze deformation ratio λ_{craze} is independent of position within the craze body suggests that fibril extension takes place by a surface drawing mechanism. Kramer assumes that this involves the flow of polymer in a strain-softened layer at the craze–bulk interface of thickness h (where h is very much less than the fibril separation) along the gradient in hydrostatic tension $\nabla\sigma_0$ between the fibril bases and the interfibrillar void tips. Then

$$\nabla\sigma_0 = \frac{2\beta S - 8\Gamma/D_0}{D_0} \tag{1}$$

where D_0 is the fibril separation, Γ is the effective surface energy at the interfibrillar void tips, S is the stress at the craze surface, and β is a factor of the order of unity.[1] Maximizing this expression with respect to D_0 gives

$$\nabla\sigma_0 = (\beta S)^2/8\Gamma \tag{2}$$

which corresponds to the maximum rate of interface advance for a given S and is taken to represent the value of D_0 that will be observed in the craze. It is further assumed by Kramer that the rate of interface advance v, and consequently the local deformation rate, may be related to $\nabla\sigma_0$ by assuming a simple power-law constitutive equation for the polymer in the strain-softened layer, so that

$$v \propto \left(\frac{h\nabla\sigma_0}{\sigma_y(T)}\right)^n \tag{3}$$

where n is an empirical constant (typically between 10 and 20) and $\sigma_y(T)$ is a yield stress.[1] As a first approximation, local deformation rates during crazing will be proportional to the applied deformation rate $\dot{\epsilon}$ during a constant strain rate tensile test, and hence, by combining eqs 2 and 3 one obtains the following expression[2] for the critical stress for craze propagation S_c at a given $\dot{\epsilon}$:

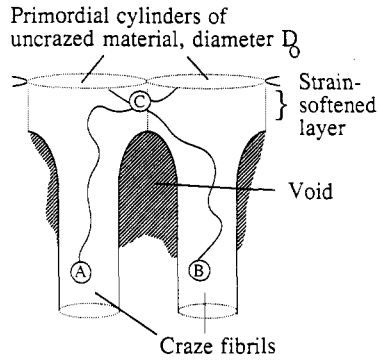

Figure 1. Schematic representation of the surface drawing mechanism during craze widening. Polymer in the thin strain-softened layer at the craze–bulk interface flows toward the fibril bases along the gradient in hydrostatic tension between the void tips and the fibril bases. The chains marked A and B and entangled at C must either break or disentangle in order to continue to move into adjacent fibrils as shown.

$$S_c \propto (\Gamma\sigma_y(T))^{1/2}(\dot{\epsilon})^{1/2n} \tag{4}$$

which contrasts with the equivalent expression for localized shear deformation[2]

$$S_{DZ} \propto \sigma_y(T)(\dot{\epsilon})^{1/n} \tag{5}$$

where the subscript DZ refers to a shear "deformation zone". This is a term used to refer to the cracklike zones of localized shear necking that characterize shear deformation in the thin-film geometry commonly used for microscopic investigations.[3–5]

Scission Crazing. To complete the model it is necessary to take into account the geometrically necessary entanglement loss during crazing as illustrated in Figure 1. The two chains A and B shown schematically are presumed to be subject to a constraint on their relative motion represented by the "entanglement point" at C. In order for the chains to continue to move into adjacent fibrils as shown, they must overcome this constraint; that is, there must be entanglement loss.[1–6] This view of entanglement as a localized constraint presupposes the entanglement network model. In this model, the network parameters are obtained from rheological data in the plateau region of rubberlike behavior shown by un-cross-linked glassy polymers above T_g, treating these data by analogy with a chemically cross-linked rubber. The

0024-9297/90/2223-3929$02.50/0

network parameters comprise the entanglement density ν_e, the spatial separation of entanglement points d_e, and the root mean square chain contour length of the polymer strands linking entanglement points l_e. In Kramer's original chain scission model for ambient temperature crazing in PS,[1] all such strands crossing the surface of the primordial cylinder of diameter D_0, representing material that would eventually be drawn into a given fibril (as shown in Figure 1), were assumed to break. Since the number of entangled strands crossing unit area is approximately $^1/_2\nu_e d_e$, then this chain breakage was accounted for by writing the effective surface energy at the void tips as

$$\Gamma = \Gamma_0 + \frac{U d_e \nu_e}{4} \tag{6}$$

where U is taken to be approximately the bond energy of the chain backbone and Γ_0 is the van der Waals surface energy of the polymer in question.

Substitution of eq 6 into eq 4 and comparison with eq 5 suggests that when ν_e is increased, the stress to propagate a scission-mediated craze will increase relative to the stress to propagate a DZ (for which no entanglement loss is necessary), and so shear deformation will tend to be the dominant mode of deformation in relatively high ν_e materials. This has been verified by experiments where ν_e has been varied systematically using PS–poly(phenylene oxide) (PPO) blends[4] and where the effective value of ν_e in PS has been increased by chemical cross-linking.[7,8] It is also found that scission crazing is independent of the chain molecular weight and favored over shear deformation by high $\dot{\epsilon}$ and low T, consistent with eqs 4 and 5.[1,2,9,10]

Disentanglement Crazing. An alternative mechanism to scission for entanglement loss is reptation.[11,12] We use "reptation" here as a generic term to refer to any mechanism of disentanglement in which a given chain may be visualized as moving along the length of a virtual confining tube representing the topological constraint on that chain arising from its interactions with neighboring chains. Thus de Gennes "classical" reptation model for diffusion[11] represents a particular case in which disentanglement occurs by Brownian motion of the chain along its confining tube. This is inappropriate to phenomena such as crazing. In crazing the chains are being forced out of their tubes by an applied force, and consequently we term this "forced reptation".[13]

McLeish et al.[13] took a simple approach in which they assumed that one end of a disentangling chain was anchored by work hardening in a filament and that the remainder of the chain was pulled out of its confining tube as the craze–bulk interface advanced. The mobility μ of a single chain is given by

$$\mu^{-1} = \mu_0^{-1} \int_0^l \exp\left(\frac{-E(s)}{kT}\right) ds \tag{7}$$

where μ_0 is the high-temperature monomeric mobility, $E(s)$ is an energy well height that models the local chain environment and is assumed to vary independently of the chain contour variable s, and l is the overall chain contour length. For a given rate of chain pullout v, which we take to be equal to the interface advance rate described earlier, the frictional force f_d acting along the chain is given by $\mu_0^{-1}v$ for each monomer, so that

$$f_d \sim \frac{v\zeta_0 M}{M_0} \tag{8}$$

where $\zeta_0 \sim \mu_0^{-1}$, and will be exponentially dependent on temperature through an Arrhenius factor $\zeta_0 = A \exp(E/RT)$, M_0 is the monomer molecular weight, and M is the total molecular weight.[13] For chain scission, the force to break a bond is approximately

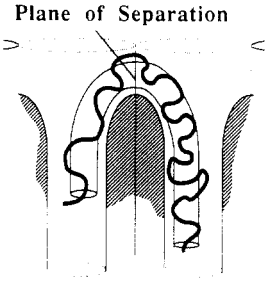

Figure 2. Kramer and Berger's model for disentanglement during craze widening. The chain shown schematically is constrained to move along a virtual tube, and as the craze–bulk interface advances, this tube is considered to be divided into two sections by the plane of separation between two fibrils as indicated. As the void tip advances, the chain either disengages by reptation from the shorter of these two sections or breaks.

$$f_b \sim U/2a \tag{9}$$

where U is the bond energy and a is the bond length.[14] If $f_d < f_b$, disentanglement will take place in preference to scission, so that, assuming v to be proportional to the applied deformation rate $\dot{\epsilon}$, one can see immediately from eqs 8 and 9 that disentanglement is favored by low $\dot{\epsilon}$, low M, and high temperature through the term ζ_0.

Kramer and Berger have subsequently developed this approach as illustrated in Figure 2.[14] They considered any molecule straddling the plane dividing two adjacent fibrils, and which must consequently disentangle for fibrillation to continue, to be divided into two sections, the shorter having a molecular weight of xM, where $x \leq {}^1/_2$. They then argued that in order for fibrillation to proceed, only the shorter section need disentangle, and so instead of eq 8 they used

$$f_d \sim \frac{2v\zeta_0 xM}{M_0} \tag{10}$$

Since x in eq 10 may take any value between 0 and $^1/_2$, the range of forces necessary for disentanglement may overlap with the force required for chain scission, so that there may be contributions to the surface energy from both.[14] A critical value of x given by

$$x_c = \frac{UM_0}{4a\zeta_0 vM} \tag{11}$$

may be obtained by equating f_b and f_d. For $x > x_c$, since $f_d > f_b$ a given chain will break rather than disentangle whereas for $x < x_c$ the chain will disentangle. Given some x_c the effective contribution to the surface tension at the void tip can then be obtained by multiplying the average force per entangled strand in the void-tip surface (as determined from eqs 10 and 11 and by making appropriate assumptions about the distribution in x) by the number of entangled strands per unit length in the surface, which is approximately $^1/_2\nu_e d_e a$. For $x_c \leq {}^1/_2$ then

$$\Gamma = \Gamma_0 + \left(1 - \int_0^{x_c}\phi(x)\,dx\right)\frac{d_e\nu_e U}{4} + \frac{d_e\nu_e a}{2}\frac{2\zeta_0 vM}{M_0}\frac{\int_0^{x_c}\phi(x)\,dx \int_0^{x_c} x\phi(x)\,dx}{\int_0^{x_c}\phi(x)\,dx} \tag{12}$$

where $\phi(x)$ is the probability density function for x. Kramer and Berger assume x to have a flat probability distribution so that $\phi(x) = 2$ for $0 < x \leq {}^1/_2$.[14] Hence, evaluating the integrals and substituting x_c back into the

resulting expression using eq 11, they obtain, for $x_c \leq 1/2$

$$\Gamma = \Gamma_0 + (1 - x_c)\frac{d_e \nu_e U}{4} \tag{13}$$

and similarly, for $x_c \geq 1/2$ (no scission)

$$\Gamma = \Gamma_0 + \left(\frac{1}{4x_c}\right)\frac{d_e \nu_e U}{4} \tag{14}$$

(Physically, of course, $x_c = 1/2$ is the limiting case although x_c in eq 11 may be greater than $1/2$.)

Effectively then, since x_c is a rapidly increasing function of T (estimates of E from melt rheology suggest typical values of the order of 100 kJ[2,14,15]), we have two limiting cases: (i) at low T, where $x_c \ll 1$, there is no significant disentanglement and eq 13 reduces to eq 6, the pure scission case, as derived previously from energy considerations; (ii) at high T, where $x_c \gg 1$, eq 14 reduces to $\Gamma = \Gamma_0$, since, in this "van der Waals" limit, there is no scission and the forces of disentanglement are sufficiently low that they no longer contribute significantly to Γ.[5,13,14] Because of the strong dependence of x_c on T, the transition between these two regimes should take place over a relatively narrow range of temperatures, and from eq 11 we expect the transition to be pushed to higher temperatures with increasing M and $\dot{\epsilon}$.

By using eq 2 to substitute for $\nabla\sigma_0$ in eq 1, it is simple to show that for the surface drawing model

$$8\Gamma = S_c D_0 \tag{15}$$

so that a knowledge of S_c and D_0 allows one to determine Γ directly.[1] Berger et al. have used low-angle electron diffraction (LAED) to obtain D_0 for thin-film crazes in high molecular weight PS (M = 1 800 000) at very low $\dot{\epsilon}$ (4×10^{-6} s^{-1}) and over a range of T from ambient temperature to just below T_g.[16] Their results confirm quantitatively the existence of and the magnitude of the change in Γ. They also confirm that the breadth of the transition is consistent with taking E to be the activation energy for disentanglement in the melt, although A, the front factor in the Arrhenius term ζ_0, is unknown and remains an adjustable parameter.

We also expect the transition from scission to disentanglement to be reflected by the behavior of the stress at which crazes first appear in an inhomogeneous sample, since it may be argued[5] that this stress will be governed by the ability of embryonic crazes to propagate beyond local stress concentrations and into the bulk; that is, it should scale as S_c or, from eq 4, as $\Gamma^{1/2}$. Hence this crazing stress should show a sharp drop corresponding to the transition from scission to disentanglement with increasing T, and this drop should occur at higher T for higher M and $\dot{\epsilon}$.

There is much experimental evidence for such behavior in a variety of materials. It was first shown by Donald[10] that the transition from crazing to shear (observed as temperature is increased in high molecular weight PS, and which is consistent with the scission mechanism) was suppressed in low molecular weight PS. This observation suggests the possibility of a molecular weight dependent drop in the crazing stress close to T_g. Subsequently we have confirmed the existence of such a drop in the crazing stress in the high-ν_e polymers poly(ether sulfone) (PES) and polycarbonate (PC).[5] The stress for scission crazing is prohibitively high in these polymers because of the dependence of S_c on ν_e through eqs 4 and 6, and if scission were the only permissible mechanism, crazing would be replaced by shear over the entire temperature range. Instead a transition from shear to crazing was observed as T was raised, which, consistent with the above discussion, was pushed to higher T with higher molecular weight average M_w and $\dot{\epsilon}$. Furthermore, in the high-temperature regime of crazing close to T_g, the crazing stress was found to be independent of M_w and weakly dependent on $\dot{\epsilon}$, which was argued to be a reflection of the M-independent van der Waals limit, $\Gamma = \Gamma_0$, in which disentanglement no longer contributes to crazing kinetics.[5] Finally, the shear to craze transition may be suppressed by light cross-linking, which is consistent with disentanglement being prevented; effectively the chains are now physically linked within their tubes and cannot escape them.[17]

Other recent evidence for disentanglement has been comprehensively summarized by Kramer and Berger and will not be discussed further.[14] Our concern here is to reexamine some of the assumptions behind the model for disentanglement crazing.

2. Effect of Multiple Crossing on Disentanglement during Crazing

Numerical calculations based on the network model and the assumption that the strands linking entanglement points are Gaussian random walks[1,18,19] suggest that approximately half of all entangled strands in PS must be broken to accommodate crazing in the scission limit (that is, approximately half the strands present cross the surface of the primordial cylinder of radius D_0 referred to in Figure 1). For stable crazes to form at all, there must be in excess of two entanglement lengths per chain,[20] and for molecular weights typical, for example, of the experimental investigations of Kramer and Berger,[2] M is greater than $5M_e$, where M_e is the entanglement molecular weight. It may readily be seen then that on average, a given chain in such a material will cross the surface of the primordial cylinder more than 2.5 times, regardless of the position of its center of gravity relative to that of the cylinder surface (although clearly the number of crossings an individual chain makes will vary from chain to chain). From the network parameters of the high entanglement density polymer PES[21] we estimate an average of ten crossings per chain (for the molecular weight averages available to us there are approximately 30 entanglements per chain).

In general then we do not expect the situation in Figure 2, that is, that of a chain trapped in a tube whose ends are embedded in adjacent fibrils and which crosses the plane between the fibrils only once. Rather, we anticipate a situation more like that illustrated in two dimensions in Figure 3, where we have represented the entanglement constraint as a regular distribution of points which the chain is unable to cross and which deforms affinely as the craze–bulk interface advances. In the remainder of this section we shall examine how this will affect the scaling associated with disentanglement-controlled crazing.

The multiple chain crossing of what will become a free surface in Figure 3 results in the chain contour velocity's being amplified along the length of the chain via a "block and tackle" mechanism as described previously by McLeish et al.[13] and Kramer and Berger.[14] If we assume all the constraints are moving at a constant average speed v, which we again take to be the craze interface advance rate, then as we move along the chain from its center, we can see that each time the chain direction reverses (that is, crosses the plane between two adjacent fibrils) its local velocity relative to its constraints will increase by a constant amount proportional to the global deformation rate. The total force in the chain is therefore a function of not only the

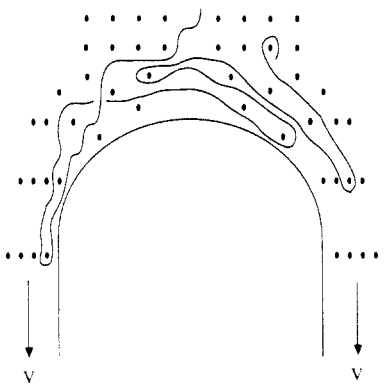

Figure 3. Effect of multiple crossings on the disentanglement mechanism. The effect of entanglement is represented by an array of point constraints that the chain is not allowed to cross and that deform affinely with the strain-softened layer as the craze–bulk interface advances. As the void advances, successive loops of the chain shown will be pulled in opposite directions as we move along the length of the chain. Thus we may approximate the behavior of the chain by the "block and tackle" mechanism.

deformation rate and molecular weight but also the total number of crossings the chain makes.

Disentanglement without Scission. Since the local chain velocity increases by a fixed amount every second time the chain crosses the plane of separation,[14] then we expect to a first approximation, as we move from the midpoint of the chain toward one of the chain ends, the local velocity relative to the continuum at the ith crossing we encounter will be $^1/_2\, iv$, and so if the molecular weight associated with each crossing is M_c, this chain segment will experience a frictional force

$$\delta f = \frac{\zeta_0 v M_c i}{2M_0} \tag{16}$$

and the total force at this point will be

$$f = \sum_{j=i}^{n_0} \frac{\zeta_0 v M_c j}{2M_0} \tag{17}$$

where $n_0 = M/2M_c$. The mean force in the chain will be

$$\langle f \rangle = \frac{1}{n_0}\sum_{i=0}^{n_0}\sum_{j=i}^{n_0}\frac{\zeta_0 v M_c j}{2M_0} = \frac{1}{n_0}\sum_{k=0}^{n_0}\frac{\zeta_0 v M_c k^2}{2M_0} \tag{18}$$

and the maximum force

$$f_{max} = \sum_{i=0}^{n_0}\frac{\zeta_0 v M_c i}{2M_0} \tag{19}$$

Assuming a large number of crossings (large n_0), we approximate the summations in the continuous limit by integrals, giving

$$\langle f \rangle \sim \frac{1}{n_0}\int_0^{n_0}\frac{\zeta_0 v M_c i^2}{2M_0}\,di = \frac{2M_c}{3M}\frac{\zeta_0 v M_c}{2M_0}\left(\frac{M}{2M_c}\right)^3 = \frac{\zeta_0 v M^2}{24M_0M_c} \tag{20}$$

$$f_{max} \sim \int_0^{n_0}\frac{\zeta_0 v M_c i}{2M_0}\,di = \frac{\zeta_0 v M_c}{4M_0}\left(\frac{M}{2M_c}\right)^2 = \frac{\zeta_0 v M^2}{16M_0M_c} \tag{21}$$

These equations are essentially the same expressions as derived by Berger and Kramer.[14]

Clearly, at some arbitrary point in time, individual chains in the active zone will be in various stages of disentanglement so that in order to compute the average force per unit area in the active zone we need to consider the average force on chains over the total time it takes to disentangle. Because the constraints are moving affinely in our model, we expect $M_c(t)$ to be increasing linearly with t from its bulk value, which we rewrite as $M_c(0)$, to a value of the order of M, at which time disentanglement will be complete. Furthermore, since the number of crossings of the plane of separation a given chain makes will be decreasing as MM_c^{-1}, then the contribution to the average force made by chains with a given M_c must be weighted by MM_c^{-1} so that from eq 20 and writing $M_c(t)$ as $M_c(0) + (M - M_c(0))\tau^{-1}t$ (where τ is a disentanglement time) our expression for $\langle f \rangle_t$ is

$$\langle f \rangle_t \sim \frac{\dfrac{\zeta_0 v M^2}{24M_0}\displaystyle\int_0^\tau \frac{\tau^2\,dt}{(M_c(0)\tau + (M - M_c(0))t)^2}}{\displaystyle\int_0^\tau \frac{\tau\,dt}{M_c(0)\tau + (M - M_c(0))t}} \sim \frac{\zeta_0 v M(M - M_c(0))}{24M_0M_c(0)\ln\left(\dfrac{M}{M_c(0)}\right)} \tag{22}$$

so that we estimate the effective surface energy to be

$$\Gamma = \Gamma_0 + \frac{d_e \nu_e a}{2}\frac{\zeta_0 v M(M - M_c(0))}{24M_0M_c(0)\ln\left(\dfrac{M}{M_c(0)}\right)} \sim \Gamma_0 + \frac{d_e \nu_e a \zeta_0 v M^2}{48M_0M_c(0)\ln\left(\dfrac{M}{M_c(0)}\right)} \tag{23}$$

for $M \gg M_c(0)$.

Finally, we note that in general, the mean molecular weight between crossings, $\langle M_c(0) \rangle$, of a single planar surface in a continuum of Gaussian chains, taken over all chains intersecting that surface, will not be independent of M. The number of independent chains crossing unit area is given by McLeish et al. as[13]

$N_a \sim$ (no. of chains contained within the volume of one chain)/(area of one chain)

which scales as $R_g{}^3M^{-1}/R_g{}^2$, where R_g is the radius of gyration of the chain.[13] Since for Gaussian chains we have that $R_g \sim M^{1/2}$, then $N_a \sim M^{-1/2}$. Now since the number of strands crossing unit area will remain constant when we vary the molecular weight, then, since the entanglement density should remain constant, we have that the mean number of crossings, $MM_c(0)^{-1}$, of an individual chain intersecting the plane of separation is inversely proportional to N_a and so $M_c(0) \sim M^{1/2}$.

Thus we expect the disentanglement contribution to Γ in the limit of the radius of gyration of the chains being very much less than the fibril separation D_0 to scale as approximately $M^{3/2}$ rather than as M suggested by eq 10. However, it should be noted that typically this limit does not apply, and so the value of $M_c(0)$ will also be strongly influenced by the craze geometry. Hence, although we might expect slightly weaker M scaling in eq 23 than would be the case if $M_c(0)$ were independent of M, we will not attempt to quantify this, and for the remainder of the paper will assume $M_c(0)$ to be constant for a given material.

Transition from Disentanglement to Chain Scission. Equation 23 does not of course take into account chain scission. In order to do this, we note that in the limit of a large amount of chain scission, immediately prior to scission, the bulk of any given chain will be stationary, and so, apart from stochastic variations, the tension in the chain will be approximately uniform. Hence we assume that

chain scission will occur randomly until f_{max} in the resulting chain fragments (eq 21) becomes of the order of or less than the force for scission. Now we note the following relationships (from eqs 20–22):

$$\langle f\rangle_t \sim \frac{\langle f\rangle}{\ln\left(\frac{M}{M_c(0)}\right)} \sim \frac{2f_{max}}{3\ln\left(\frac{M}{M_c(0)}\right)} \tag{24}$$

These clearly remain valid as $\langle f\rangle_t$ approaches the point where we begin to get scission, that is, where $f_{max} \sim U/2a$, so that the onset of chain scission should occur when $f_{max} \sim U/2a$, and

$$\langle f\rangle_t \sim \frac{U}{3a\ln\left(\frac{M}{M_c(0)}\right)} \tag{25}$$

and

$$\Gamma \sim \Gamma_0 + \frac{d_e\nu_e U}{4}\frac{2}{3\ln\left(\frac{M}{M_c(0)}\right)} \tag{26}$$

We now consider the regime where scission is also taking place. First, we define a critical molecular weight M_{crit} such that

$$\frac{U}{2a} = f_{max}(M_{crit}) = \frac{\zeta_0 v M_{crit}^2}{16 M_0 M_c(0)} \tag{27}$$

and we assume that once scission is taking place then its effect will be such that the molecular weight of the chain fragments will be of the order of M_{crit} (we shall qualify this assumption later). From simple energetic arguments (cf. eq 6), since the number of scission events per chain will be approximately M/M_{crit}, we have that

$$\Gamma = \Gamma_0 + \frac{d_e\nu_e U}{4}\frac{M}{M_{crit}}\frac{M_c(0)}{M} + \Gamma_d \tag{28}$$

where Γ_d represents additional contributions to Γ from disentanglement of the chain fragments and is expected to tend to zero as M_{crit} tends to $M_c(0)$ (i.e., when all the strands crossing the plane of separation undergo chain scission). In this limit, eq 28 gives eq 6, that is, the expression derived by Kramer for pure scission.[1]

We know that once the chain fragments are disentangling, f_{max} in these chains will be approximately $U/2a$ so that from eq 24, noting that only a proportion $1 - M_c(0)/M_{crit}$ of the entangled strands will be disentangling, we have that in the limit $M_c(0) \ll M_{crit}$

$$\Gamma_d \sim \left(1 - \frac{M_c(0)}{M_{crit}}\right)\frac{d_e\nu_e U}{4}\frac{2}{3\ln\left(\frac{M_{crit}}{M_c(0)}\right)} \tag{29}$$

or more precisely, making use of eq 22, that

$$\Gamma_d \sim \left(1 - \frac{M_c(0)}{M_{crit}}\right)\frac{d_e\nu_e U}{4}\frac{2(M_{crit} - M_c'(0))}{3M_{crit}\ln\left(\frac{M_{crit}}{M_c'(0)}\right)} \tag{30}$$

where

$$M_c'(0) = M_c(0)\frac{1 - \frac{M_c(0)}{M_{crit}}}{1 - \frac{M_c(0)}{M}}$$

This last equation takes into account that the effective value of $M_c(0)$ will be decreasing as the amount of scission increases, because subsequent to scission the number of chain ends per unit volume will have increased. Rewriting eq 23 in terms of M_{crit}, we get our complete expressions for Γ:

$$\Gamma = \Gamma_0 + \frac{d_e\nu_e U}{4}\frac{M_c(0)}{M_{crit}} + \frac{d_e\nu_e U}{4}\left(1 - \frac{M_c(0)}{M_{crit}}\right)\frac{2(M_{crit} - M_c'(0))}{3M_{crit}\ln\left(\frac{M_{crit}}{M_c'(0)}\right)}; \quad M > M_{crit} \tag{31a}$$

$$\Gamma = \Gamma_0 + \frac{d_e\nu_e U}{4}\frac{2(M - M_c(0))}{3M\ln\left(\frac{M}{M_c(0)}\right)}\left(\frac{M}{M_c(0)}\right)^2; \quad M \le M_{crit} \tag{31b}$$

We now return to the question of the effective molecular weight of the chain fragments in the scission regime. We originally assumed random scission, on the basis of the further assumption that where there was large-scale scission, the tension in the chains would be approximately uniform immediately prior to scission. However, in the limit of very few scission events per chain, a large proportion of each chain will be mobile and hence the maximum force in the chain will tend to be close to its midpoint, so that as f_{max} approaches $U/2a$, the chains will tend to break in half. Hence we expect the effective molecular weight of the resulting fragments to be $M_{crit}/2$ rather than M_{crit}. Thus, noting that $\langle f\rangle_t$ will in general scale approximately with the molecular weight squared (eq 22), we expect Γ_d to be one-quarter of the value implied by eqs 29 and 30 as M_{crit} approaches M.

This presents the possibility of there being a discontinuity in Γ at the transition. That is, as we decrease T, there will be a sudden catastrophic drop in Γ at the onset of scission. It follows therefore that the crazing stress, which scales with $\Gamma^{1/2}$, will also show such an abrupt change. This is a direct consequence of the fact that the entangled strands crossing the plane of separation are not independent of each other, and will tend to break in the center, and is consequently beyond the scope of earlier models.

3. Experimental Section

We have examined crazes in PS (supplied by Polymer Laboratories Ltd.) and PES (Victrex, supplied by ICI plc). The PS samples were monodisperse with molecular weights of 127 000 and 1 150 000. Commercially available PES, on the other hand, being a condensation polymer, is highly polydisperse (with a polydispersity of the order of 2). Two differing molecular weight distributions were made use of, which we term here M1 and M4 to be consistent with the nomenclature of Davies and Moore.[22] The molecular weight averages of M1 and M4 were approximately 47 000 and 69 000 respectively. In order to increase this range somewhat, we carried out fractionation in the manner described by Davies and Moore,[22] to separate the low molecular weight tail from M1, using dimethylformamide/ethanol as a solvent/nonsolvent system for PES. For the weight fractions obtained, we have estimated the molecular weight average to be 25 000 from data for the molecular weight distribution of M1 given by Davies and Moore.[22]

Thin films of the order of 0.4 μm in thickness were made by letting a drop of a solution of the polymer in question fall from a syringe onto a rotating glass slide (the speed of rotation of the slide controlled the film thickness). When the solvent had evaporated, the resulting film was floated off on a water bath and picked up on copper grid previously coated with the same polymer, to which the film was bonded, after drying, by a short exposure to the appropriate solvent vapor.[23,24] The solvents were toluene

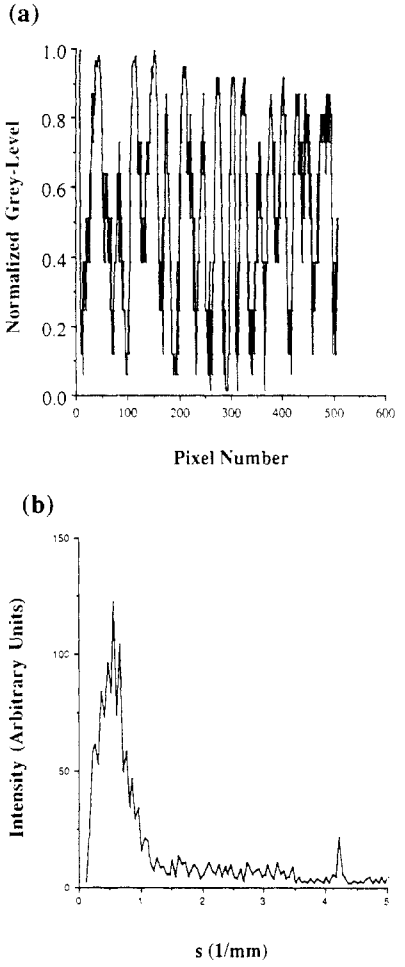

Figure 4. (a) A gray-level profile taken perpendicular to the fibril direction in a TEM micrograph of a PS craze and (b) the corresponding fast Fourier transform.

and cyclohexanone at 40 °C for PS and PES, respectively. When the films had been bonded to the grids, they were placed in a vacuum oven for 12 h at T_g - 20 °C in order to dry them and also to physically age them and hence to suppress shear deformation.[5,25]

We have used the spin-casting method since it is economical in terms of the amount of polymer required and, in particular, since, by attaching a 0.2-μm filter to the syringe, we were able to produce dust-free drops and hence dust-free films relatively efficiently. The films, on their copper grids, were then strained at a constant strain rate of 4×10^{-6} s^{-1}, on a heating stage, while being observed with an optical microscope that could be operated in both reflected and transmitted light. The strains at which crazes first appeared in the samples at various temperatures were recorded, and subsequent to deformation and removal from the straining rig, the individual grid squares were examined by transmission electron microscopy (TEM).

Using 1-D fast Fourier transforms (FFTs) of digitized TEM images of crazes, we estimated the mean fibril separation using the method of Yang and Kramer.[26] Digitization was carried out by using a black and white television camera with a microscope lens attachment from which discrete 512 × 256 pixel images, with 64 gray-level resolution, could be dumped onto a framestore using the Oxford Framestore Applications Ltd. package running on an Olivetti M24 PC (personal computer). This enabled gray-level profiles to be obtained perpendicular to the fibril direction in a given craze image such as in Figure 4a. The input to the FFT program (also run on the PC) consisted of a composite gray-level profile consisting of 2048 points. The fibril spacing D_0 was estimated from an average of four FFTs from a given micrograph (this procedure was sufficient to obtain reproducible results), taking $D_0 \sim s_p^{-1}$, where s_p is the distance from the origin in reciprocal space of the first maximum in the FFT (see Figure 4b).[26] Each data point represents an average value of D_0 estimated from several different micrographs.

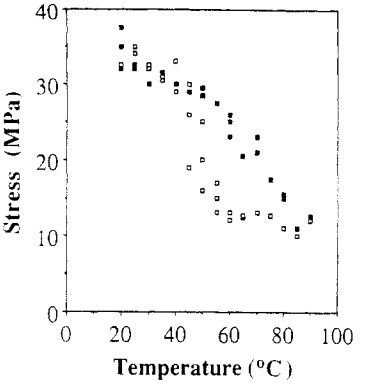

Figure 5. The stress to craze in PS at a strain rate of 4×10^{-6} s^{-1} plotted against temperature for two molecular weights, 127 000 (open squares) and 1 150 000 (filled squares).

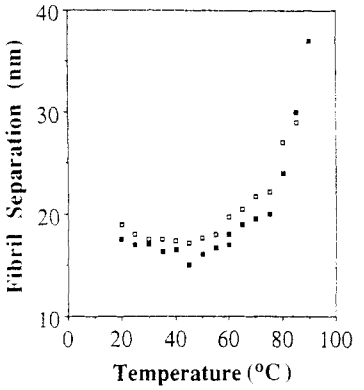

Figure 6. The fibril separation PS crazes strained at 4×10^{-6} s^{-1} plotted against temperature for two molecular weights, 127 000 (open squares) and 1 150 000 (filled squares).

4. Results and Discussion

We have calculated the stress S_c at which the crazes in our samples were formed from our strain data by assuming a linear stress–strain curve up to the crazing strain ϵ_c. The conversion was carried out assuming a tensile modulus $E \sim 2900$ MPa at 273 K with $dE/dT \sim 4.5$ MPa K^{-1} for PS and $E \sim 2700$ MPa at 273 K with $dE/dT \sim 6$ MPa K^{-1} for PES.[21] We then made use of eq 15 to approximate Γ at the craze void tips. To begin with, we consider each set of results in turn. It should be noted that there is considerable scatter in the results, which might typically lead to a 20% uncertainty in S_c, as can be seen from the figures. For PES, previous data[21] in macroscopic tests have shown that despite the possibility of shear deformation, the stress–strain curves remain linear for temperatures ≤150 °C. This implies that the conversion of crazing strain to stress via a temperature-dependent Young's modulus is valid.

PS Results. In Figure 5 we show the stress to craze S_c in PS for M = 127 000 and for M = 1 150 000 as a function of T. As T increased from room temperature, both the high- and the low-M results showed a weak decrease in S_c, and S_c remained approximately independent of M. At ca. 40 °C, S_c for M = 127 000 began to drop more sharply and then leveled off at ca. 10 MPa above 60 °C. A similar drop in S_c occurred at ca. 70 °C for M = 1 150 000.

The D_0 results are given in Figure 6: D_0 remains approximately constant at between 15 and 20 nm over much of the temperature range, consistent with earlier measurements of D_0 using LAED,[16] and then begins to rise with T as T approaches T_g, this rise commencing at ca. 60 °C for both molecular weights.

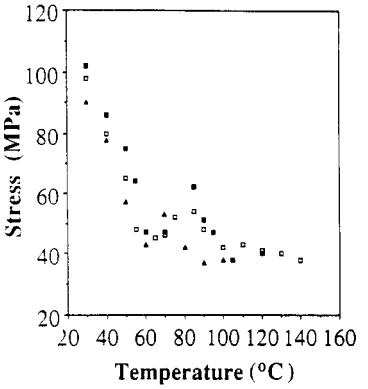

Figure 7. The stress to craze in PES at a strain rate of 4×10^{-6} s^{-1} plotted against temperature for three molecular weight averages, M4 (filled squares), M1 (open squares), and a low molecular weight fraction with an estimated molecular weight average of 25 000 (filled triangles).

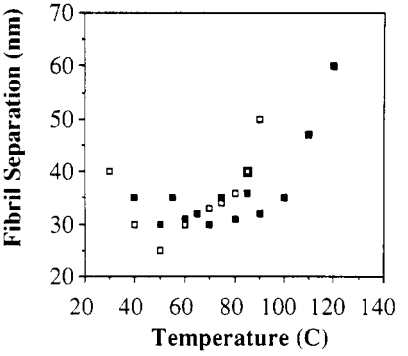

Figure 8. The fibril separation in PES crazes strained at 4×10^{-6} s^{-1} plotted against temperature for two molecular weight averages, M1 (open squares) and M4 (filled squares).

PES Results. Results for S_c are given in Figure 7 for the different molecular weight averages of PES. There is a marked drop in S_c for deformation onset as the temperature is increased, associated with a transition from shear deformation to crazing, as has been observed previously in PES and PC (polycarbonate)[5] (our samples showed only shear deformation at room temperature). S_c then appeared to reach a minimum for all the molecular weights at ca. 60 °C, and a slight maximum just above this temperature, before falling again with T to level off at ca. 38 MPa. This maximum was at a slightly higher temperature for M1 and M4 than for the low molecular fraction, but the difference was small. It had not been detected in previous observations of the strain to craze in PES,[5] carried out at a higher strain rate of ca. 10^{-2} s^{-1}. However, there was a suggestion of a similar peak in a previous series of measurements carried out on M1 at a strain rate of 6×10^{-5} s^{-1}, also given in ref 5.

D_0 data are given in Figure 8 for M1 and M4, the data for the low molecular weight tail being unobtainable using TEM because of beam damage, the crazes rapidly tearing open. D_0 drops slowly with T at low temperatures, from ca. 40 to 30 nm between 40 and 70 °C. Above 70 °C D_0 begins to rise rapidly for M1, reaching 60 nm by 90 °C, beyond which temperature the crazes become too unstable to examine. For M4, the rise is less steep, D_0 reaching a value of 60 nm at 120 °C.

Comparison of the Results with the Model. We can estimate all the quantities in eq 31 for both PES and PS with the exception of ζ_0; while data are available for the activation energy for ζ_0 from melt data, the front factor A in the expression $\zeta_0 = A \exp(E/RT)$ is not well-known. Although the use of melt data in the glassy state is unsatisfactory, in the absence of data below T_g we follow the lead of Kramer and Berger[14] in using these figures. For PS, Kramer and Berger[14] estimate a value of 1.7×10^{-28} N s m^{-1} and using this value and a value of 159 kJ mol^{-1} for the activation energy E, we obtain the curves given in Figure 9 (values for the other parameters are also given in the literature[1,14]). These curves predict a drop in Γ with T that is approximately independent of M in the mixed scission/disentanglement regime and then a discontinuous change in slope at the transition to the disentanglement only regime, where Γ is strongly dependent on M.

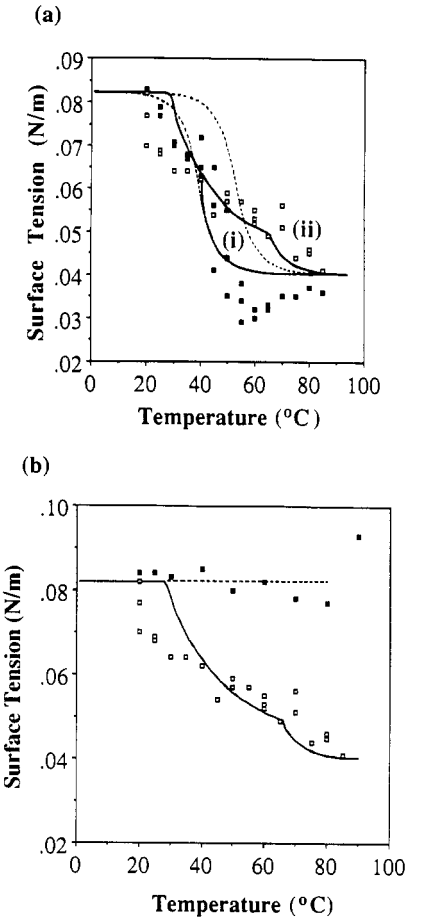

Figure 9. (a) Predicted $\Gamma(T)$ curves for PS at a strain rate of 4×10^{-6} s^{-1}. The solid curves are our predictions for (i) $M = 127\,000$ and (ii) $M = 1\,150\,000$ and the dashed curves are Kramer and Berger's predictions for comparison. We have also shown our experimental results for Γ for $M = 127\,000$ (filled squares) and $M = 1\,150\,000$ (open squares). (b) Predicted $\Gamma(T)$ curves for PS, $M = 1\,150\,000$, at a strain rate of 4×10^{-6} s^{-1} (solid curve) and 10^{-2} s^{-1} (dashed curve) compared with data for the same strain rates.

We can compare our predictions with values for Γ estimated from our values for D_0 and S_c via eq 15 and also shown in Figure 9. Although the basic assumption of our model, that the number of crossings any given chain makes of the plane of separation should be large, becomes questionable for $M = 127\,000$ where there are on average approximately three crossings per chain, the agreement between the predicted and the observed positions of the transitions is reasonable. In particular, the apparent shape of the $\Gamma(T)$ curves at low strain rates is better represented than the predictions of Kramer and Berger's model,[14] for which we give typical curves in Figure 9a for comparison. For $M = 1\,150\,000$, the block and tackle mechanism gives a very much broader transition region than the original Kramer and Berger model, which is consistent with our results and also consistent with the results of Berger et

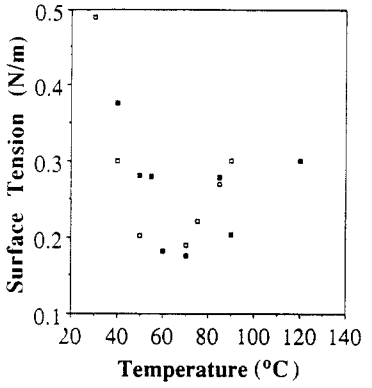

Figure 10. Effective surface tension Γ at the craze void tips in PES strained at 4×10^{-6} s^{-1} as calculated from the D_0S_c values given in Figures 7 and 8 for two molecular weight averages, M1 (open squares) and M4 (filled squares).

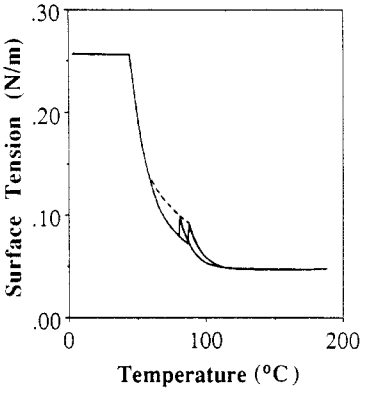

Figure 11. Predicted Γ(T) curves for PES. The curves are for molecular weight averages (i) M_w = 47 000 and (ii) M_w = 69 000. The solid lines represent the behavior expected if the effective M of the disentangling chains undergoes a twofold reduction at the onset of scission, and the dotted lines represent the behavior predicted if this correction is not made.

al. for M = 1 800 000.[16] Indeed, these results suggest that the transition region extends to even lower T than we have predicted, and we speculate that this may be a consequence of the relaxation of the tube constraint when a large number of scission events are taking place.

At high strain rates we expect relatively little dependence of Γ on T, since disentanglement will be replaced by scission over most of the temperature range. In Figure 9b, we give some data for M = 1 150 000 obtained at a strain rate of 10^{-2} s^{-1} and these suggest that the scission to disentanglement transition is completely suppressed under such conditions.

Figure 10 gives values of Γ for PES M1 and M4 calculated from our S_c and D_0 data at a strain rate of 6×10^{-5} s^{-1} via eq 15. To model these results we have used a value of 114 kJ mol^{-1} for the activation energy[15] and a value for A of ca. 10^{-22} N s m^{-1}, which is consistent with our observation of a steep drop in Γ between 40 and 60 °C. We give model curves for M1 and M4 calculated with these values, and estimates of the other parameters (see ref 21), in Figure 11. (Note that while it is possible, if tedious, to take into account the molecular weight distribution when calculating the average force in the chains at the void tips, we find that it makes no significant difference to the final form of Γ(T) if we assume monodispersity and take M equal to M_w). Again these curves indicate a drop in Γ with T that is initially independent of molecular weight in the mixed scission/disentanglement regime and then shows a discontinuous change in slope at the transition to the disentanglement only regime where Γ is molecular weight dependent. First we note that the quantitative agreement between the model and the results is not as good for PES as for PS. Γ appears to be underestimated at low temperatures, and the high-T increase in Γ in Figure 10 is unaccounted for. There is some evidence of similar increase in Γ in PS very close to T_g, but in PES it appears to commence more than 100 °C below T_g. In PS, the effect is likely to be a consequence of changes in the drawing behavior at the craze surface, as a result of softening at high T, and in particular, a systematic increase in the thickness of the strain-softened layer h (see eq 3) above ca. 80 °C.[14] In PES, however, the extreme fragility of the craze microstructure at high T may have lead to an apparent value for D_0 that is too high, because of radiation-induced fibril breakdown during TEM examination (indeed, above the maximum T for which we give data for D_0, the crazes were too fragile to examine with TEM at all). Fibril damage may also account in part for the relatively poor quantitative agreement between our PES results and the model predictions at relatively low T.

One striking feature of the results for S_c in PES is the maximum in $S_c(T)$ observed between ca. 60 and 100 °C (Figure 7). We speculated on the possibility of such a maximum at the end of section 2 and have shown in Figure 11 the behavior we would expect for Γ if a catastrophic reduction in effective molecular weight of disentangling chains does take place at the onset of chain scission. If we then assume that the stress at which crazes appear in our samples is given by eq 4, that is, that the rate-determining step in craze formation in our samples is craze propagation, then since $S_c \sim \Gamma^{1/2}$, the predicted behavior of Γ in Figure 11 does reflect the qualitative behavior of S_c in our PES samples (in our results for Γ the maxima corresponding to the maxima in S_c appear to be masked by the uncertainty in D_0). Possibly as a result of scatter in the data, no clear maxima were observed for PS, and since the correction to the model curves is both small and only likely to be valid in the immediate vicinity of the temperature at which scission first occurs, we have omitted it from Figure 9. It should be noted that the monodisperse PS would be expected to give a very sharp discontinuous transition occurring over a few degrees at most. A rise in stress over such a very narrow temperature range could easily be missed.

There is some evidence that the model does not account fully for the variation of S_c with M at a given temperature in PES. In the results given here in Figure 7, there is little difference in the T at which the maxima in S_c occur in M1 and M4, which is consistent with the model (note that whereas there is a factor of 10 difference between the two molecular weights of PS used here, the ratio of the two PES molecular weights used here is only of the order of 1.5). However, there does appear to be a small, but significant dependence of the magnitude of S_c on M_w in the scission/disentanglement regime for PES which is not predicted. Moreover, in earlier results[5] for PES obtained at a strain rate of 10^{-2} s^{-1}, and in which the transition to disentanglement crazing was pushed to relatively high T, S_c was a far stronger function of M_w than can be accounted for in terms of the model. Thus the model appears to provide an incomplete description of the behavior of these polydisperse materials.

We speculate that there may be a link between the dependence of S_c on M in polydisperse materials and the low molecular weight tail of the molecular weight distribution in question and that this is most likely a plasticization effect owing to the relatively high diffusiv-

ity of the very low molecular weight chains (possibly involving tube renewal). Brown has discussed in some detail the effect of plasticization on the surface drawing mechanism and concludes that even very small degrees of plasticization can have a dramatic effect on crazing kinetics through the effect of plasticization on the thickness of the strain-softened layer at the craze–bulk interface.[27] It has also been suggested that diffusion of relatively low molecular weight polybutadiene (PBD) can mediate crazing in blends of PS and very low proportions of PBD, the PBD being concentrated in localized reservoirs and then diffusing along the craze–bulk interface when a craze nucleates at the reservoir.[28] Finally, comparison of measurements of the stress profiles in polydisperse PS and monodisperse PS crazes has suggested that the fibril drawing rate at a given stress may be profoundly affected by the presence of low molecular weight chains.[29] However, it is not clear why the influence of these low molecular weight chains should be apparently much stronger in the high strain rate PES data of ref 5 than in the data given in this paper.

5. Conclusions

We have modeled the crazing stress as a function of temperature in terms of a block and tackle mechanism for disentanglement of polymer chains, taking into account the possibility of effective molecular weight reduction in the regime of mixed disentanglement and scission, owing to multiple crossing by a given chain of the plane of separation between two adjacent fibrils.

We have also investigated the crazing strain as a function of molecular weight and temperature in thin films of PS and PES mounted on copper grids at a strain rate of 4×10^{-6} s^{-1}. on the basis of our results we argue that the block and tackle mechanism for disentanglement during crazing accounts well for the behavior of PS. For PES, the quantitative agreement between our results and the predictions is not good. However, we have been able to account for the appearance of maxima in the $S_c(T)$ curves for PES, which we predicted to coincide with the onset of crazing mediated by disentanglement alone as the temperature is raised. Finally, we find that in PES, although the molecular weight dependence of the positions of these peaks in S_c on the T axis may be accounted for well by the model, there appears to be an additional molecular weight dependence in S_c which we believe to be a plasticization effect relating to the extent of the low molecular weight tail in a given grade. This is an effect for which a description lies outside our simple ideas on disentanglement.

Acknowledgment. We gratefully acknowledge the support of ICI plc during the course of this work and E. J. Kramer and L. L. Berger for valuable discussions and allowing us to preview ref 14.

References and Notes

(1) Kramer, E. J. *Adv. Polym. Sci.* **1983**, *52/53*, 1.
(2) Berger, L. L.; Kramer, E. J. *Macromolecules* **1987**, *20*, 1980.
(3) Donald, A. M.; Kramer, E. J. *J. Mater. Sci.* **1981**, *16*, 2967.
(4) Donald, A. M.; Kramer, E. J. *Polymer* **1982**, *23*, 461.
(5) Plummer, C. J. G.; Donald, A. M. *J. Polym. Sci., Polym. Phys. Ed.* **1989**, *27*, 235.
(6) Donald, A. M.; Kramer, E. J. *J. Polym. Sci., Polym. Phys. Ed.* **1982**, *20*, 899.
(7) Henkee, C. S.; Kramer, E. J. *J. Polym. Sci., Polym. Phys. Ed.* **1985**, *22*, 721.
(8) Berger, L. L.; Kramer, E. J. *J. Mater. Sci.* **1988**, *23*, 3536.
(9) Fellers, J. F.; Kee, B. F. *J. Appl. Polym. Sci.* **1974**, *18*, 2355.
(10) Donald, A. M. *J. Mater. Sci.* **1985**, *20*, 263.
(11) De Gennes, P.-G. *J. Chem. Phys.* **1971**, *55*, 572.
(12) Doi, M.; Edwards, S. F. *J. Chem. Phys.* **1971**, *55*, 1789, 1802.
(13) McLeish, T. C. B.; Plummer, C. J. G.; Donald, A. M. *Polymer* **1989**, *30*, 1651.
(14) Kramer, E. J.; Berger, L. L. *Adv. Polym. Sci.* **1990**, *91/92*, 1.
(15) James, S. G. Ph.D. Thesis, Cambridge, 1988.
(16) Berger, L. L.; Buckley, D. J.; Kramer, E. J.; Brown, H. R.; Bubeck, R. A. *J. Polym. Sci., Polym. Phys. Ed.* **1987**, *25*, 1679.
(17) Plummer, C. J. G.; Donald, A. M. *J. Mater. Sci.*, in press.
(18) Kuo, C. C.; Phoenix, S. L.; Kramer, E. J. *J. Mater. Sci. Lett.* **1985**, *4*, 459.
(19) Kramer, E. J. *Polym. Eng. Sci.* **1984**, *24*, 761.
(20) Yang, A. C.-M.; Kramer, E. J.; Kuo, C. C.; Phoenix, S. L. *Macromolecules* **1986**, *19*, 2010.
(21) Plummer, C. J. G.; Donald, A. M. *J. Appl. Polym. Sci.*, in press.
(22) Davies, M.; Moore, D. R. ICI plc: Internal Report, 1987.
(23) Beahan, P.; Bevis, M.; Hull, D. *J. Mater. Sci.* **1973**, *8*, 162.
(24) Lauterwasser, B. D.; Kramer, E. J. *Philos. Mag.* **1979**, *20*, 469.
(25) Donald, A. M.; Kramer, E. J. *J. Mater. Sci.* **1982**, *17*, 1871.
(26) Yang, A. C.-M.; Kramer, E. J. *J. Mater. Sci.* **1986**, *21*, 3601.
(27) Brown, H. R. *J. Polym. Sci., Polym. Phys. Ed.* **1989**, *27*, 1273.
(28) Brown, H. R.; Argon, A. S.; Cohen, R. E.; Gebizioglu, O. S.; Kramer, E. J. *Macromolecules* **1989**, *22*, 1002.
(29) Donald, A. M.; Kramer, E. J. *Polymer* **1983**, *24*, 1063.

Registry No. PS, 9003-53-6.